Complex Metal Halide Oxides (3). Structural Characteristics and Catalytic Performance of Lanthanum-Substituted X1X2 Type Complex Bismuth Chloride Oxides

Sui Wen Lin and Wataru Ueda[*,#]

Department of Environmental Chemistry and Engineering, Tokyo Institute of Technology, 4259 Nagatsuta, Midori-ku, Yokohama 226-0087

(Received November 16, 1998)

The replacement of bismuth ions with lanthanum ions in the cation-oxygen sheets of layered $Bi_3SrCl_3O_4$ catalyst promoted the activity for the oxidative dehydrogenation of ethane prominently. The structure of $Bi_{3-n}La_nSrCl_3O_4$ remained in the X1X2 structure by the replacement untill the lanthanum ion content (n) was in excess of 0.75, and the value of a of the sub-unit cell and the value of c representing thickness of the layer structure were changed reversely. The Rietveld analysis of the $Bi_{2.25}La_{0.75}SrCl_3O_4$ catalyst revealed that the thickness of the double chlorine sheet decreased when the coordination number of lanthanum ion facing the double chlorine sheet increased from 8 to 9, suggesting that the interaction between the metal-oxide sheet and the chlorine sheet became stronger. This is supported by a reduced binding energy of chlorine in $Bi_{2.25}La_{0.75}SrCl_3O_4$ observed by XPS analysis. The activation of structural chlorine into a radical form is promoted by the replacement with lanthanum ion, which turns out to cause an increase of the oxidation activity of ethane.

The oxidative dehydrogenation of ethane is of both applied and fundamental importance, because ethane is predominant in natural gas and the products such as ethene are precursors to consumer products. If ethane can be dehydrogenated in high yields, it will become an alternate feedstock. A large number of catalysts have been studied for the oxidative dehydrogenation of ethane.[1—15] For activating ethane oxidatively, we designed catalysts containing chlorine to activate the C–H bond of ethane.[16] Thus, for this purpose, we synthesized complex metal chloride oxides, in which chlorine ions are fixed in the crystalline structure. These structural catalysts showed a good catalytic performance for selective oxidative dehydrogenation of ethane.[17] Among them $Bi_3SrCl_3O_4$ catalysts having X1X2 type structure gave the highest selectivity to ethene and exhibited a good structural stability under the reaction condition.[16,17]

In the X1X2 structure, metal–oxygen sheets were separated by single chlorine layers and double chlorine layers alternately.[16] It was proven that the chlorines between the metal–oxygen sheets are a key element in the C–H bond activation of ethane to ethene.[16] In this work, the metal–oxygen sheets of the $Bi_3SrCl_3O_4$ catalyst were modified by the introduction of lanthanum ion in order to increase the catalytic performance. There are two reasons for this modification: one is that the ionic radius of lanthanum ion is similar to that of bismuth ion, which avoids any structural change by the replacement of bismuth ion with lanthanum ion;[18] the other reason is that the lanthanum oxide has a higher ability for oxygen activation.[19] The relationship between structural deformation and increase of catalytic activity is discussed.

Experimental

Catalyst Synthesis. $Bi_{3-n}La_nSrCl_3O_4$ (n = 0—1) were synthesized by solid-state reaction of stoichiometric mixtures of bismuth oxide, bismuth chloride oxide (BiClO), lanthanum chloride oxide (LaClO), and strontium chloride. All chemicals used for the preparation were commercially available reagent grade except LaClO, which was prepared by the solid-state reaction between lanthanum oxide and lanthanum chloride at 1123 K for 20 h in air. Lanthanum-substituted layered complex bismuth chloride oxide catalysts were prepared by heating the given mixture at 1173 K for 20 h in alumina crucibles.

Characterization of Catalysts For ascertaining phase purity and to determine sub-unit cell dimensions, powder X-ray diffraction data for the $Bi_{3-n}La_nSrCl_3O_4$ catalysts were collected using a diffractometer (Mac Science MXP[18]) and auto-monochromated Cu $K\alpha$ radiation (50 kV, 300 mA). Data suitable for structure solution and refinement were collected over the range 20°—120° in 0.02° steps. Data analysis was carried out by the Rietveld method using the RIETAN program.[20] An X-ray electron spectrometer (Shimadzu ESCA-3200) was used to characterize the state of chlorine between the metal–oxygen sheets. The binding energies were calibrated to the Au $4f_{7/2}$ value (83.8 eV).

Catalytic Reaction Apparatus The catalytic reaction was carried out in a fixed-bed reactor at atmospheric pressure. The reactor was constructed of high-purity alumina tube having 11 mm i.d. Two single-walled sealed alumina tubes (6 mm o.d.) were inserted, one from each side of the reactor, these were for reducing

Present address: Department of Materials Science and Engineering, Science University of Tokyo in Yamaguchi, 1-1-1 Daigakudori, Onoda, Yamaguchi 756-0084.

the empty volumes. One of the sealed ends which was inserted into the catalysts zone served as a thermowell for measuring the reaction temperature, while the other was for supporting the catalysts in the reactor. The catalysts were loaded in the middle part of the reactor, and the amount of catalyst used, unless indicated otherwise, was 2g, which was diluted by quartz sand (catalyst : quartz sand = 1 : 1 (wt)). The feed gas was controlled with mass flow controllers (KOFLOC, model 3510) which have a ±1.5% FS precision. The total flow rate was 50 ml min^{-1} (ethane : oxygen : nitrogen = 1 : 4 : 15), unless otherwise noted. Reaction products were separated with Porapak Q, T and Molecular 13X, and were analyzed using a gas chromatograph equipped with a thermal conductivity detector (GL Science). The data were collected by an auto-sampling system and analyzed by using V-Station software. Nitrogen in the feed was used as an internal standard for the calculation of the conversion and selectivity. The conversion and selectivity were calculated based on the reacted ethane; the carbon and oxygen balances were nearly 100%. It was confirmed that no reaction took place when the reaction was carried out without oxygen or catalyst at the standard reaction conditions indicated above.

Results and Discussion

Structural Phase of Lanthanum-Substituted Complex Bismuth Chloride Oxide Catalysts. The layered bismuth chloride oxide catalysts, which show a variety of structures,[21—24] generally consist of cation–oxygen layers (cationic) associated with the tetragonal PbO structure, alternating with single or multiple sheets (anionic) of halide ions. Bismuth ion in the metal–oxygen sheet can be replaced by other cations. As indicated in the recent work,[16,17] the X1X2 structure can be synthesized by the replacement of strontium ion in the $[Bi_2O_2]$ sheets. The structure of the $Bi_3SrCl_3O_4$ catalyst has been refined by the Rietveld method,[16] in which metal–oxygen sheets were separated by single chlorine layers and double chlorine layers alternately. Moreover, it is possible to substitute bismuth ion for other cations having large ionic radius, such as the rare-earth element lanthanum ion. Here, the bismuth ions in the metal–oxygen sheet $[M_2O_2]$ (M: Bi, Sr) of $Bi_3SrCl_3O_4$ catalyst were replaced by lanthanum ions, and the change of the structure of the $Bi_3SrCl_3O_4$ was investigated. The general composition of the lanthanum-substituted complex bismuth chloride oxide catalysts is given by $Bi_{3-n}La_nSrCl_3O_4$, the nominal components used in the preparation of the catalysts. It was confirmed by X-ray diffractiometry that the catalysts remained in the X1X2 type structure during the replacement with lanthanum ion to a certain degree ($n \leq 0.75$) Table 1. The XRD patterns for $Bi_{3-n}La_nSrCl_3O_4$ catalysts are shown in Fig. 1. The diffraction pattern for $Bi_3SrCl_3O_4$ catalyst showed monophasic in the X1X2 structure. As the extent of the substitution increased (n = 0.25, 0.5, 0.75), the diffraction patterns showed the same phase as X1X2, but peaks shifted. For example, the reflections of (101) (32.2 deg.) shifted to lower angle obviously. When the lanthanum content (n) increased to 1, additional diffraction peaks were observed besides those of the X1X2 structure. However, the phase giving these peaks has not been identified yet. The changes in the sub-unit cell parameter of $Bi_{3-n}La_nSrCl_3O_4$ catalysts are shown in Fig. 2. On increasing the lanthanum content, the value a along the sheet in the sub-unit cell increased from 3.937 Å (n = 0) to 3.973 Å (n = 0.75). Although the value a change was very faint because the ionic radius of lanthanum ion was slightly larger than that of bismuth, it is clear that the lanthanum ion invaded into the cation–oxygen sheet by the substitution. On

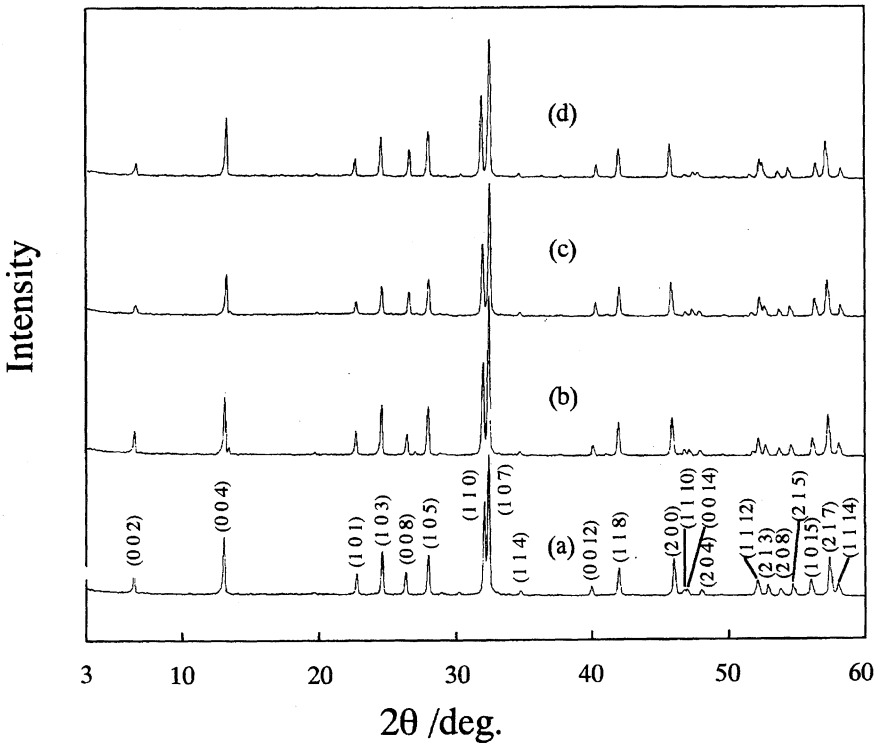

Fig. 1. The XRD patterns of $Bi_{3-n}La_nSrCl_3O_4$ catalysts. (a): n = 0, (b): n = 0.25, (c): n = 0.5, (d): n = 0.75.

Table 1. Preparative Condition and Surface Area of Lanthanum-Substituted Bismuth Strontium Chloride Oxide Catalysts

Catalyst composition	Reactant	Structural phase	Surface area $m^2 g^{-1}$
$Bi_3SrCl_3O_4$	$SrCl_2+Bi_2O_3+BiClO$	X1X2	0.2
$Bi_{2.75}La_{0.25}SrCl_3O_4$	$SrCl_2+Bi_2O_3+0.75BiClO+0.25LaClO$	X1X2	0.3
$Bi_{2.5}La_{0.5}SrCl_3O_4$	$SrCl_2+Bi_2O_3+0.5LaClO$	X1X2	0.4
$Bi_{2.25}La_{0.75}SrCl_3O_4$	$SrCl_2+Bi_2O_3+0.25BiClO+0.75LaClO$	X1X2	0.3
$Bi_2LaSrCl_3O_4$	$SrCl_2+Bi_2O_3+LaClO$	X1X2+IP[a)]	—

a) Impurity phase.

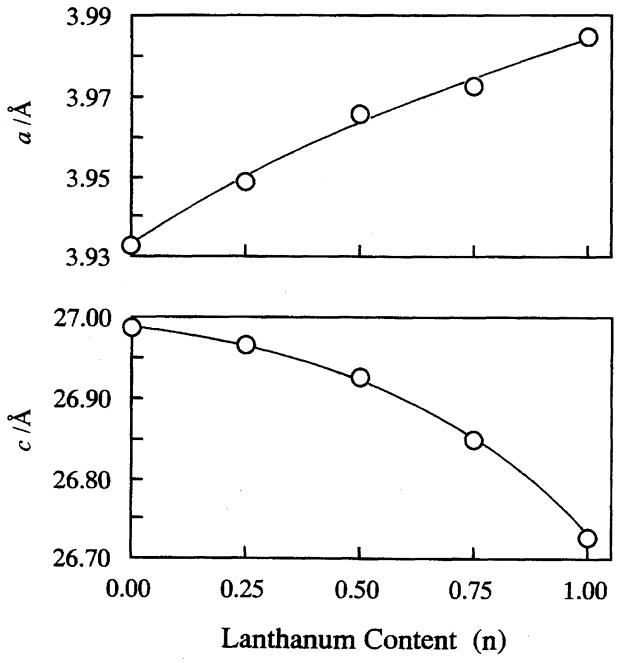

Fig. 2. Variation of lattice parameters by the replacement of Bi with La in $Bi_{3-n}La_nSrCl_3O_4$ catalysts.

the other hand, the value of *c* representing the thickness of the layer structure decreased prominently from 27.017 to 26.849 Å. Such a preferential variation in the sub-unit cell parameters is very interesting. The contraction of the thickness of the layer structure indicates that the interaction between the metal–oxygen sheet and the chlorine sheet becomes stronger.

Rietveld Analysis for the $Bi_{2.25}La_{0.75}SrCl_3O_4$ Catalyst. Although the $Bi_{3-n}La_nSrCl_3O_4$ catalysts remained in the X1X2 structure, *a* and *c* values of sub-unit cell of the catalysts showed the opposite variations. To explain these changes, the lanthanum-substituted bismuth chloride oxide catalyst was analysized by the Rietveld method. We refined the structure of the $Bi_{2.25}La_{0.75}SrCl_3O_4$ catalyst. Then the structures were compared between the $Bi_{2.25}La_{0.75}SrCl_3O_4$ catalyst and the $Bi_3SrCl_3O_4$ catalyst. The structure details of $Bi_{2.25}La_{0.75}SrCl_3O_4$ catalyst finally determined by Rietveld method are given in Table 2. First, the powder pattern of $Bi_{2.25}La_{0.75}SrCl_3O_4$ was indexed to be the same as the $Bi_3SrCl_3O_4$ catalyst, giving a primitive tetragonal cell. The reflection condition *hkl* was $h+k+l=2n$, and physical tests on non-centro-symmetry were negative, so that the centrosymmetric space group *I4/mmm* was chosen as the space group of $Bi_3SrCl_3O_4$ catalyst. Final Rietveld plots for the X-ray refinement are given in Fig. 3. The refinement proceeded straightforwardly, which allowed an anisotrropic temperature factor for the structural atoms; the final refined atomic parameters for the $Bi_{2.25}La_{0.75}SrCl_3O_4$ catalyst are shown in Table 3. Lanthanum ions occupied the site of bismuth ion impartially, and the anticipated Sillen-type $[M_2O_2]$ (M: Bi, La, Sr) layers can be seen. The structural model of $Bi_{2.25}La_{0.75}SrCl_3O_4$ is similar to that of $Bi_3SrCl_3O_4$. The metal–oxygen sheets were separated by single chlorine layers and double chlorine layers alternately. According to the results of Rietveld analysis, the structural deformation of lanthanum-substituted X1X2 type complex bismuth chloride oxides is discussed below.

Table 2. Crystal Data and Refinement of $Bi_{2.25}La_{0.75}SrCl_3O_4$ Catalyst

Crystal System	Tetragonal
Space group	*I4/mmm*
Cell parameters	$a=3.9725(1)$ Å
	$c=26.849(4)$ Å
2θ range	20—120°
No. reflections	260
No. points	5000
R_{wp} R_p	10.24% 7.16%

The selected bond lengths are listed in Table 4. It indicates that the interatomic distances of M–O and M–Cl in the $Bi_{2.25}La_{0.75}SrCl_3O_4$ catalyst are longer than those in $Bi_3SrCl_3O_4$ catalyst; this can be attributed to the larger ionic radius of lanthanum ion. In the X1X2 structure, metal ions lie in the depressions between four oxygen ions. It is understandable that introducing the lanthanum ion can result in a

Table 3. Final Atomic Parameters for $Bi_{2.25}La_{0.75}SrCl_3O_4$

Atom	Site	*g*	*x*	*y*	*z*
Bi(1)	4e	0.75	0	0	0.0731(1)
Bi(2)	4e	0.375	0	0	0.3376(2)
La(1)	4e	0.25	0	0	0.0731(1)
La(2)	4e	0.125	0	0	0.3376(2)
Sr(1)	4e	0.5	0	0	0.3376(2)
O (1)	8g	1.0	0.5	0	0.111(1)
Cl(1)	4e	1.0	0	0	0.2109(9)
Cl(2)	2b	1.0	0	0	0.5

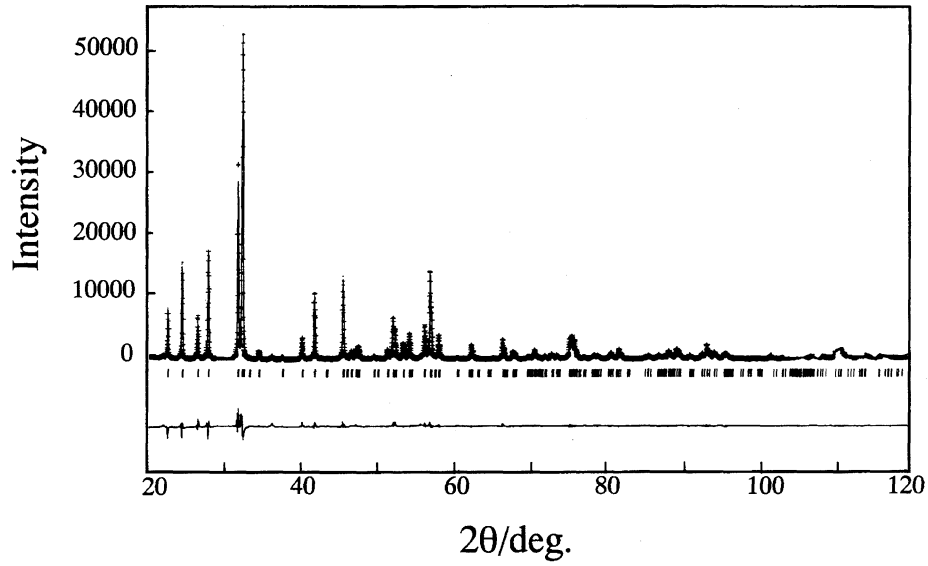

Fig. 3. Final Rietveld for $Bi_{2.25}La_{0.75}SrCl_3O_4$ catalyst, X-ray data.

Table 4. Interatomic Distance in Angstroms

$Bi_{2.25}La_{0.75}SrCl_3O_4$[a)]		$Bi_3SrCl_3O_4$	
M(1)–O	2.24	Bi(1)–O	2.18
M(1)–Cl(2)	3.43	Bi(1)–Cl(2)	3.39
M(2)–O	2.41	Bi(2)–O	2.36
M(2)–Cl(1)	3.10	Bi(2)–Cl(1)	3.08

a) M: Bi, La, and Sr.

little change in size of the $Bi_{3-n}La_nSrCl_3O_4$ catalysts (lattice parameter a increase), so the value of a along the sheet in the sub-unit cell slightly increased by the introduction of lanthanum ion.

The position of the chlorine of double chlorine layer is decided by the space coordinate of Cl(1) (0, 0, z). According to the structural symmetry relationships, the perpendicular distance between the double chlorine layer can be calculated using the space coordinate of Cl(1) and the value of c by the following equation:

$$\Delta d = c(0.5 - 2z),$$

where Δd is the the perpendicular distance between the double chlorine layer, c is the lattice parameter, and z is the space coordinate of Cl(1).

The space coordinate z of Cl(1) in the structure of the $Bi_3SrCl_3O_4$ catalyst is 0.205, and that in the structure of $Bi_{2.25}La_{0.75}SrCl_3O_4$ catalyst is 0.210. The calculated result showed that the distance of the double chlorine layer in the $Bi_{2.25}La_{0.75}SrCl_3O_4$ catalyst is 2.10 Å which is smaller than that of the $Bi_3SrCl_3O_4$ catalyst (2.43 Å). It is clear that the thickness of the double chlorine layer becomes thinner by the replacement. The metal ions in $Bi_3SrCl_3O_4$ catalyst show a 8-coordination; a square of four oxygens is located above the metal ion and a square of four chlorines below. The double chlorine layers are connected by the Van der Waals bond. On the other hand, if the bismuth site was replaced by the lanthanum ion, the lanthanum ion can interact with the second chloride layer in the double chlorine sheet as shown in Fig. 4, because lanthanum ion can exist in 9-coordination structure. In fact, the distance between the metal ion (Bi/La) and the second chloride layer in the double chloride sheet was measured to be 3.40 Å (the distance of the dotted line) in the structure of the $Bi_{2.25}La_{0.75}SrCl_3O_4$ catalyst, as indicated in Fig. 4, and Bi–Cl distance was measured to be 3.77 Å in the structure of $Bi_3SrCl_3O_4$. The increased coordination number is the reason that the thickness of the double chloride layers becomes thinner.

However, the unit cell of X1X2 structure contains two double chlorine layers. So if the contraction of c axis ($Bi_{2.25}La_{0.75}SrCl_3O_4$) was attributed to the variation of the thickness of the double chlorine sheets only, the contraction of c axis ($Bi_{2.25}La_{0.75}SrCl_3O_4$) would be 0.66 Å, but in this catalyst, only a 0.17 Å contraction was observed as indicated in the result of lattice parameters. The reason for this is very simple; the replacement of lanthanum ion into the metal–oxygen sheet increases value a of sub-unit cell because of its larger ionic radius and therefore the thickness of the metal–oxygen sheet also increased. As a consequence,

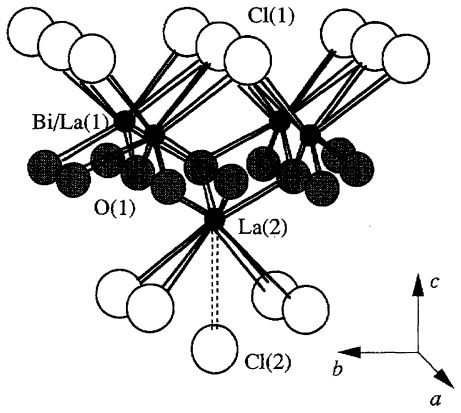

Fig. 4. The local structure of $Bi_{2.25}La_{0.75}SrCl_3O_4$ catalyst.

the thickness of the *c* axis of the lanthanum-substituted X1X2 layered complex bismuth chloride oxide catalysts decreased at the double chlorine sheet and the interaction between the oxide and double chlorine sheet became stronger.

XPS Spectra of Cl_{2p} for the Lanthanum-Substituted X1X2 Complex Bismuth Chloride Oxide Catalysts. Changes of Cl_{2p} binding energies by the replacement of bismuth ion with lanthanum ion in the metal–oxygen sheet of $Bi_3SrCl_3O_4$ catalyst were investigated. The Cl_{2p} spectra of the $Bi_3SrCl_3O_4$ and $Bi_{2.25}La_{0.75}SrCl_3O_4$ catalysts are shown in Fig. 5. The peak position and FWHM of the $Bi_3SrCl_3O_4$ and $Bi_{2.25}La_{0.75}SrCl_3O_4$ catalysts are summarized in Table 5. These spectra show a doublet $2p_{3/2}$ and $2p_{1/2}$ with a split of 1.6 eV. The Cl_{2p} peaks of $Bi_3SrCl_3O_4$ were at 197.7 eV ($Cl_{2p3/2}$) and 199.3 eV ($Cl_{2p1/2}$). The Cl_{2p} peaks of $Bi_{2.25}La_{0.75}SrCl_3O_4$ appeared as broad peaks shifted to lower binding energy, 197.1 eV ($Cl_{2p3/2}$) and 198.7 eV ($Cl_{2p1/2}$), respectively, indicating that the chlorine ions were perturbed by the presence of the lanthanum ion in the metal–oxygen sheet of the $Bi_3SrCl_3O_4$ catalyst. This trend can be seen in Fig. 6, where variation in the Cl_{2p} binding energy of the $Bi_{3-n}La_nSrCl_3O_4$ catalysts is shown. With the increase of lanthanum content, binding energies of Cl_{2p} decreased. It should be noted that the $La_{4p3/2}$ peak of $Bi_{2.25}La_{0.75}SrCl_3O_4$ was at 197 eV. This peak and the Cl_{2p} peak overlapped, but according to the $La_{3d5/2}$ and $La_{4p3/2}$ peaks of La_2O_3 and

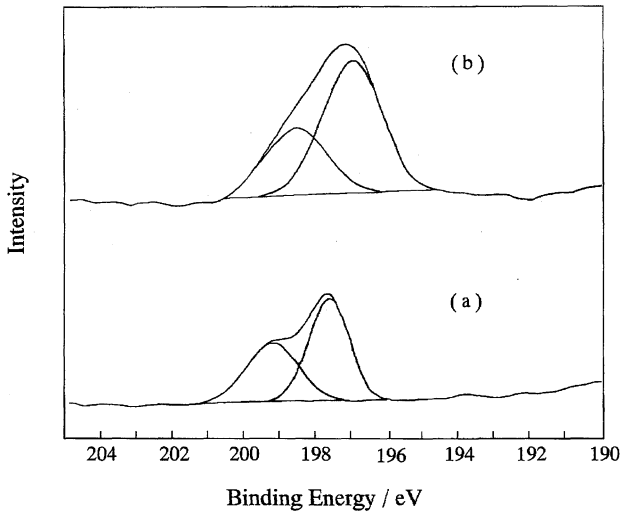

Fig. 5. The Cl_{2p} XPS spectra of $Bi_3SrCl_3O_4$ (a) and $Bi_{2.25}La_{0.75}SrCl_3O_4$ (b).

Table 5. XPS Data of Cl_{2p} for $Bi_3SrCl_3O_4$ and $Bi_{2.25}La_{0.75}SrCl_3O_4$ Catalysts

Catalyst	Binding energy/eV	FWHM/eV
$Bi_3SrCl_3O_4$		
$Cl_{2p3/2}$	197.7	1.3
$Cl_{2p1/2}$	199.3	1.7
$Bi_{2.25}La_{0.75}SrCl_3O_4$		
$Cl_{2p3/2}$	197.1	1.9
$Cl_{2p1/2}$	198.7	2.0

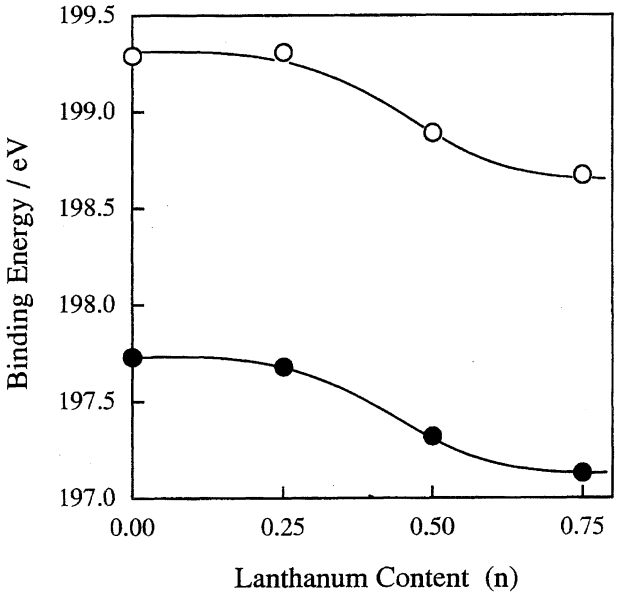

Fig. 6. Variation of binding energy of Cl_{2p} in the $Bi_{3-n}La_nSrCl_3O_4$ catalysts (○: $Cl_{2p1/2}$, ●: $Cl_{2p3/2}$).

to the $La_{3d5/2}$ peak of $Bi_{2.25}La_{0.75}SrCl_3O_4$, it is understandable that the $La_{4p3/2}$ peak of $Bi_{2.25}La_{0.75}SrCl_3O_4$ was very weaker than Cl_{2p} (in the XPS spectra of $Bi_{2.25}La_{0.75}SrCl_3O_4$ catalyst, the area ratio of $La_{4p3/2}$ peak to Cl_{2p} peak was 0.08). It also can be said that the variance of Cl_{2p} peak has no direct relation with the $La_{4p3/2}$ peak. According to the result of the structural analysis, lanthanum ion and bismuth ion occupied the same sites, the coordination number of metal ion facing the double chlorine sheet changed from 8 (4O+4Cl) to 9 (4O+5Cl), and the contraction of double chlorine sheet made the distance between the chlorine ions in the double chlorine sheet decrease from 3.7 Å ($n = 0$) to 3.5 Å ($n = 0.75$). Therefore, it may be considered that the interaction between the double chlorine sheet and the metal (lanthanum)–oxygen sheet decreases the binding energy of the electron of chlorine ions.

On the other hand, the single chlorine sheet has no obvious changes, since there is no significant structural change in the environment of the chlorine. Therefore, by the replacement the spectra of Cl_{2p} became broader. As shown in Fig. 5, we can see that these are superimposed spectra, but it is difficult to separate the peaks more meticulously because the peaks appear simply broad. From the Rietveld and XPS analysis, it is suggested that the chlorine ion existing in the $Bi_{3-n}La_nSrCl_3O_4$ catalysts can release the electron more easily than that in the $Bi_3SrCl_3O_4$ catalyst under the catalytic oxidation condition. Then we can expect that the introduction of lanthanum ions promotes the catalytic activity.

The Promotion Effect of Lanthanum Ion in the $Bi_3SrCl_3O_4$ Catalyst for the Oxidative Dehydrogenation of Ethane. The promotion effect of lanthanum ion on the oxidative dehydrogenation of ethane is shown in Fig. 7. In order to obtain a stable catalytic reaction, the catalysts were calcined at 900 °C. Therefore the catalysts were well-sintered, and their surface areas were less than 0.5 $m^2\ g^{-1}$(BET

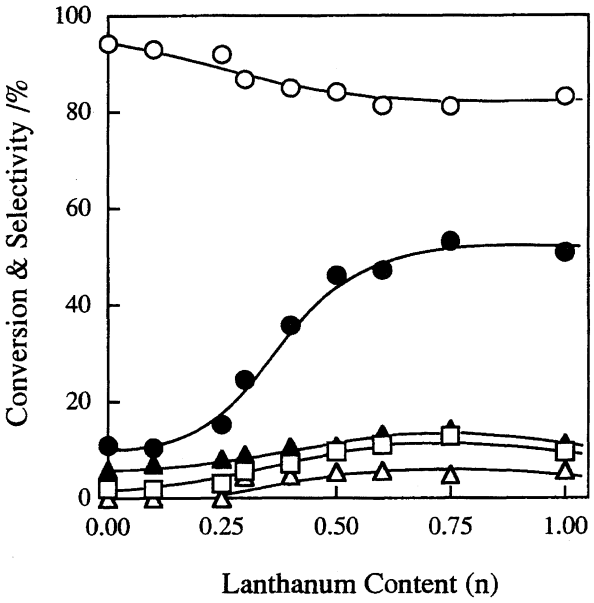

Fig. 7. The oxidative dehydrogenation of ethane over $Bi_{3-n}La_nSrCl_3O_4$ catalysts at 640 °C. □: Conv. O_2, ●: Conv. C_2H_6, ○: Sel. C_2H_4, △: Sel. CO, ▲: Sel. CO_2.

method) as shown in Table 1. All the catalysts exhibited good performance for the formation of ethene as shown in Fig. 7. The $Bi_3SrCl_3O_4$ catalyst showed a high selectivity to ethene, but the conversion of ethane was low, about 10% conversion of ethane. The introduction of lanthanum ion ($n = 0.25$) has given 15% conversion of ethane. When $n > 0.25$, the conversion of ethane increased markedly. The $Bi_{2.25}La_{0.75}SrCl_3O_4$ catalyst is about four times more active than the $Bi_3SrCl_3O_4$ catalyst for the oxidation of ethane and a maximum ethane conversion of 53% was observed over $Bi_{2.25}La_{0.75}SrCl_3O_4$ catalyst. However, the selectivity to ethene slightly decreased with the increase of lanthanum content. For example, the selectivity decreased to 81% ($n = 0.75$) from 96% ($n = 0$).

As listed in Table 1, the surface area of the catalysts has not changed significantly by the replacement. This is consistent with the XRD patterns of $Bi_{3-n}La_nSrCl_3O_4$ catalysts, which showed that the peaks of X1X2 phase did not become broader and less intense. It is, therefore, apparent that the size of the crystalline particle has not obviously changed. It can be said that the surface area of the catalysts is not a important factor for the increased conversion. For the oxidative dehydrogenation of ethane, it can be considered that the increased catalytic activity can be attributed to the structural deformation of $Bi_{3-n}La_nSrCl_3O_4$ catalysts and the enhanced oxidation ability of the cation–oxygen sheet by the introduction of lanthanum ions.

As indicated in the XPS results, the binding energies of Cl_{2p} decreased with the increase of lanthanum content (Fig. 6), and we can see that this change coincides with that of the catalytic activity (Fig. 7) very well. Therefore it is reasonable to assume that the enhancement of the catalytic acivity by the introduction of lanthanum is caused by the change of the thickness of the double sheet along with a change of electronic state of the structural chlorine in the double sheet. For the great enhancement of the catalytic acivity by the introduction of lanthanum, a possible explanation based on the above observation is as follows: The lattice chloride ion can release electrons to the metal–oxygen sheets to become a radical chlorine by the thermal process. The radical chlorine thus formed would be capable of activating ethane to ethyl radicals. The ethyl radicals immediately convert into ethene. In this point of view, the activation of chlorine is very important for oxidative dehydrogenation of ethane on the chloride-containing surface of metal chloride oxide-based catalysts.

With the replacement, the selectivity to ethene decreased slightly. One may think that the decreased selectivity is attributed to the increase of the conversion of ethane. Here, we investigated dependencies of the conversion and selectivity to ethene on the contact time for $Bi_{2.25}La_{0.75}SrCl_3O_4$ catalyst, and the results are shown in Fig. 8. While the conversion increased as the W/F increased, the selectivity to ethene is almost independent of the conversion of ethane; when the conversion of ethane increased to 53% from 8%, the selectivity to ethene remained about 81%. It is apparent that the conversions of ethane to ethene and to CO_x proceed separately in this system and the oxidation of ethene is very slow.

Therefore, the decrease of selectivity to ethene shown in Fig. 7 can be attributed to the lanthanum ions in the metal–oxygen sheets. A destructive oxidation reaction was mainly obtained over pure LaClO catalyst. So it can be considered that the lanthanum ion in the metal–oxygen sheets can form activated oxygen species for the destructive oxidation of ethane. We already explained that the activation of chlorine ion is promoted by the introduction of lanthanum

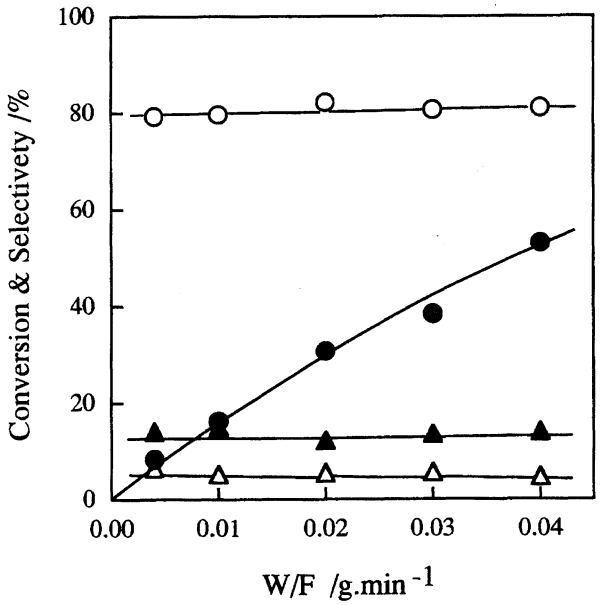

Fig. 8. The oxidative dehydrogenation of ethane as function of contact time over $Bi_{2.25}La_{0.75}SrCl_3O_4$ catalyst. Reaction temperature 640 °C, total flow rate 50 ml min^{-1}, $C_2H_6 : O_2 : N_2 = 1 : 4 : 15$. ●: Conv. C_2H_6, ○: Sel. C_2H_4, △: Sel. CO, ▲: Sel. CO_2.

ion into the metal–oxygen sheet, but the existence of lanthanum ions in the metal–oxygen sheet would also result in the complete oxidation of ethane at the same time. Thus, the selectivity to ethene slightly decreased with the increase of lanthanum content.

The activation energies of the $Bi_{3-n}La_nSrCl_3O_4$ catalysts ($n \leq 0.75$) were investigated. The reaction strictly obeys the Arrhenius equation. The activation energies are summarized in Fig. 9. The $Bi_3SrCl_3O_4$ catalyst showed a 248 kJ mol^{-1} of activation energy, but that of the $Bi_{2.25}La_{0.75}SrCl_3O_4$ catalyst decreased to 168 kJ mol^{-1}. A linear relationship between $\ln A$ and E_a was obtained, as shown in Fig. 9. This indicates a compensation effect in the oxidative dehydrogenation of ethane over $Bi_{3-n}La_nSrCl_3O_4$ catalysts. As reported earlier,[16] the catalytic performance strongly depends on the environment of chloride ion in the structure. It was also suggested that the surface chlorine having radical character has to be generated repeatedly in the catalytic oxidation cycle by the prompt action of oxygen species from molecular oxygen activated on the cation–oxygen sheet. On this basis, the compesation effect suggests that the activation process of surface chlorine by the action of metal–oxygen sheets is a key step in the course of the oxidation and is strongly influenced by the structure around chlorine.

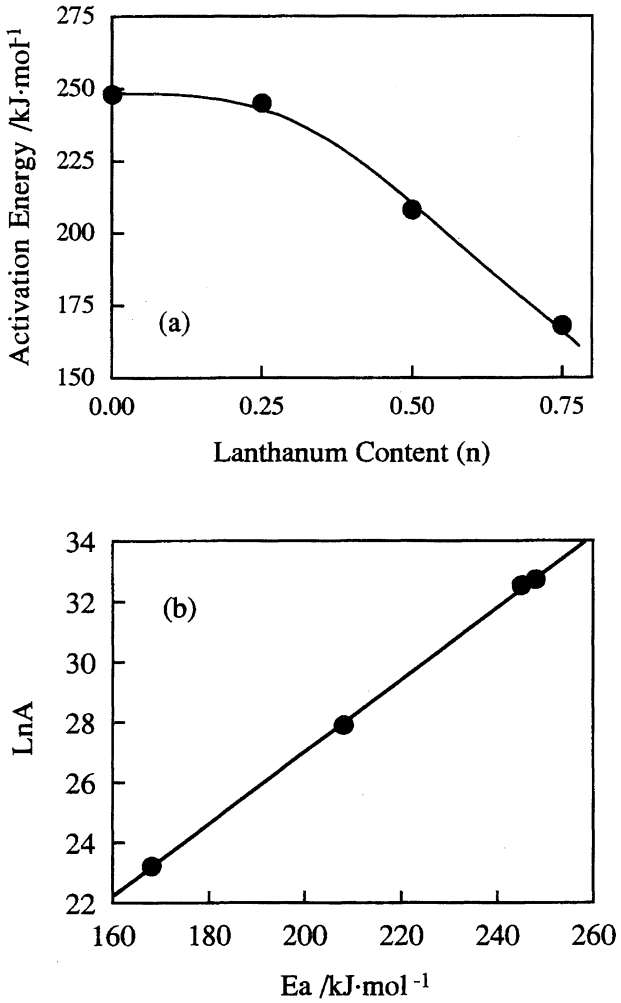

Fig. 9. The activation energy (a) and compensation effect (b).

Conclusion

With the replacement of lanthanum ion in the cation–oxygen sheet of $Bi_3SrCl_3O_4$ catalysts, the $Bi_{3-n}La_nSrCl_3O_4$ ($n \leq 0.75$) catalyst remained in the X1X2 structure, while the activity for the oxidative dehydrogenation of ethane were promoted prominently. The Rietveld analysis of the $Bi_{2.25}La_{0.75}SrCl_3O_4$ catalyst revealed that the increase of the coordination number of the metal ion facing the double chlorine sheet from 8 to 9 resulted in a decrease of the thickness of the double chlorine sheet. The interaction between the metal–oxide sheet and the chlorine sheet became stronger; this is supported by a reduced binding energy of chlorine in $SrBi_{2.25}La_{0.75}O_4Cl_3$. It is suggested that the activation of structural chlorine into a radical form is promoted by the replacement with lanthanum ion, which turns out to cause the increase of the oxidation activity of ethane.

This work has been carried out as a research project of The Japan Petroleum Institute commissioned by the Petroleum Energy Center with the subsidy of The Ministry of International Trade and Industry.

References

1) Y. Murakami, K. Otsuska, Y. Wada, and A. Morikawa, *Bull. Chem. Soc. Jpn.*, **63**, 340 (1990).
2) Y. Schuurman, V. Ducarme, T. Chen, W. Li, C. Mirodatos, and G. A. Martin, *Appl. Catal. A*, **163**, 227 (1997).
3) C. T. Au and X. P. Zhou, *J. Chem. Soc., Faraday Trans.*, **93**, 485 (1997).
4) X. P. Zhou, Z. S. Chao, J. Z. Luo, H. L. Wan, and K. R Tsai, *Appl. Catal. A*, **133**, 263 (1995).
5) H. Swaan, A. Toebes, K. Seshan, J. G. Van Ommen, and J. R. H. Ross, *Catal. Today*, **13**, 629 (1992).
6) S. J. Conway and J. H. Lunsford, *J. Catal.*, **113**, 513 (1991).
7) Vasant R. Choudhary, Shafeek A. R. Mulla, and Vilas H. Rane, *J. Chem. Technol. Biotechnol.*, **71**, 167 (1997).
8) S. Trautmann and M. Baerns, *J. Catal.*, **136**, 613 (1992).
9) K. Wada, Y. Watanabe, F. Saitoh, and T. Suzuki, *Appl. Catal. A*, **88**, 23 (1992).
10) E. M. Kennedy and N. W. Cant, *Appl. Catal. A*, **87**, 171 (1992).
11) K. Otsuka, Y. Uragami, and M. Hatamo, *Catal. Today*, **13**, 667 (1992).
12) R. Burch and E. M. Crabb, *Appl. Catal. A*, **97**, 49 (1993).
13) G. Yi, T. Hayakawa, A. G. Andersen, K. Suzuki, S. Hamakawa, A. P. E. York, M. Shimizu, and K. Takehira, *Catal. Lett.*, **38**, 189 (1996).
14) S. Bernal, G. A. Martin, P. Moral, and V. Perrichon, *Catal. Lett.*, **6**, 231 (1990).
15) S. Hong and J. B. Moffat, *Catal. Lett.*, **40**, 1 (1996).
16) S. W. Lin, Y. C. Kim, and W. Ueda, *Bull. Chem. Soc. Jpn.*, **71**, 1089 (1998).
17) W. Ueda, S. W. Lin, and I. Tohmoto, *Catal. Lett.*, **44**, 241 (1997).
18) B. Aurivillius, *Chem. Scr.*, **24**, 125 (1984).
19) W. Ueda, T. Isozaki, F. Sakyu, S. Nishiyama, and Y. Morikawa, *Bull. Chem. Soc. Jpn.*, **69**, 485 (1996).

20) Y. I. Kim and F. Izumi, *J. Ceram. Soc. Jpn.*, **102**, 401 (1994).
21) L. G. Sillen, *Z. Anorg. Allg. Chem.*, **242**, 41 (1939).
22) L. G. Sillen, *Z. Anorg. Allg. Chem.*, **246**, 115 (1941).
23) L. G. Sillen and E. Jornstad, *Z. Anorg. Allg. Chem.*, **250**, 367 (1942).
24) L. G. Sillen, *Naturwissenschaften*, **22**, 318 (1942).